

Magnetically Enhanced Microflow Cytometer for Bead-based Immunoaffinity Measurements in Whole Blood Samples



Scientific thesis for the attainment of the academic degree
Master of Science (M.Sc.)
of the Department of Electrical and Computer Engineering
at the Technical University of Munich.

Supervised by Dr.-Ing. Mathias Reisbeck
Prof. Dr. rer. nat. Oliver Hayden

Submitted by Johann Alexander Brenner
Weisbergerstraße 5a
85053 Ingolstadt
03662733

Submitted on December 4th, 2020 at Munich

Contents

1 Theory	1
1.1 Microfluidics	1
1.1.1 Incompressibility of Fluid Flows	1
1.1.2 Flow and Shear in Microchannels with Viscous Fluids	2
1.1.3 Force Equilibrium of Microbeads	4
1.2 Surface Chemistry	10
1.2.1 Surface Oxidation Methods.....	10
1.2.2 Silane Chemistry	14
1.2.3 Carbodiimide Crosslinker Chemistry	15
1.2.4 Microscopic Particle Surface Physics	17
1.2.5 The Biotin-Avidin-System	17
1.3 Magnetoresistive Sensing	17
List of Abbreviations.....	20
List of Figures	23
List of Tables	24
Bibliography	26
Statement	41

1. Theory

The main measurement principle of a microfluidic channel in connection with a giant magneto resistance (GMR)-Sensor has been already described and characterized exhaustively by Helou [1], Reisbeck [2] and others. [3], [4] Therefore, this theoretical part will focus on (bio-)physical aspects of a cell rolling motion inside a microfluidic channel and surface modification chemistry.

1.1. Microfluidics

1.1.1. Incompressibility of Fluid Flows

The main experiments of this work were carried out in microfluidic environments, which exhibit favorable properties compared to common macrofluidic systems. From a fluid-mechanical standpoint, shrinking the scales makes interfacial as well as electrokinetic phenomena much more significant, and reduces the importance of pressure and gravity.[5] However, electrodynamics, chemistry and fluid dynamics are inextricably intertwined, so that fluid flow can create electric fields (and vice versa), with a degree of coupling driven by the surface chemistry. Many of the resulting phenomena arise or can be explained by the conservation of mass described by the continuity equation (Eq. 1.1) and the conservation of momentum described by the Cauchy-Momentum equation (eq. 1.4) and the resulting Navier-Stokes equation(eq. 1.8).

$$\frac{\partial}{\partial t} \iiint \rho \, dV = - \iint \rho \mathbf{u} \cdot \vec{n} \, dA \quad (1.1)$$

$$\nabla \cdot \mathbf{u} = 0 \quad (1.2)$$

$$\frac{\partial}{\partial t} \iiint \rho \mathbf{u} \, dV = - \iint \rho \mathbf{u} \mathbf{u} \cdot \vec{n} \, dA + \iint \boldsymbol{\tau} \cdot \vec{n} \, dA + \iiint \sum_i \mathbf{f}_i \, dV \quad (1.3)$$

$$\rho \frac{\partial \mathbf{u}}{\partial t} + \rho \mathbf{u} \cdot \nabla \mathbf{u} = \nabla \cdot \boldsymbol{\tau} + \sum_i \mathbf{f}_i \quad (1.4)$$

$$(1.5)$$

The foremost assumption in fluid dynamics is termed “incompressibility”, when density gradients are negligibly small to assume a uniformity thereof. This leads to a significant

simplification of the conservation equations, because any transfer from kinetic to internal energy can be ignored.¹ This equation states that the mass of a control volume (in this case the volume integral over the density (ρ)) can only change by the mass flux over its unit outward normal (\vec{n}) transported by the flow field (\mathbf{u}). For constant ρ the mass does never change over time. This finding and the application of Gauss's theorem yields the conservation of mass in an incompressible fluid. (Eq. 1.2)

1.1.2. Flow and Shear in Microchannels with Viscous Fluids

The final equation and Gauss's theorem can now be applied to the conservation of momentum relation. (Eq. 1.3) Integration yields then the Cauchy momentum equation which states that any change in momentum inside a control volume ($\rho \frac{\partial \mathbf{u}}{\partial t}$) is caused by convective transport for or to the volume ($\rho \mathbf{u} \cdot \nabla \mathbf{u}$), surface stresses ($\nabla \cdot \boldsymbol{\tau}$), and the volumetric net body forces (\mathbf{f}_i) such as gravity or electrostatics.

Hereby, the surface stress surface stress tensor ($\boldsymbol{\tau}$) can be further decomposed into the pressure stress tensor ($\boldsymbol{\tau}_{pressure}$) and viscous stress tensor ($\boldsymbol{\tau}_{viscous}$) as shown in the equations 1.6. Characteristically, the pressure related contributions act normal and independently from \mathbf{u} whereas viscous forces act normal and tangential, and are dependent on \mathbf{u} . The $\boldsymbol{\tau}_{pressure}$ can therefore be expressed by a scalar pressure acting in every spatial dimension which is spanned by the identity.

The viscous stresses however can not be described by a continuum equation but only by a constitutive relation of atomistic processes. The underlying fundamental model of Newton's mechanics assumes that dynamic viscosity (η) is neither dependent on any velocity nor on the strain rate. Therefor, fluids which satisfy this condition are called "Newtonian fluids". Omitting special cases such as shear-thinning, -thickening or complex colloidal fluids such as undilute blood, η is the scalar proportionality that relates the strain rate to surface stress.[5] This is captured in the equation $\boldsymbol{\tau}_{viscous} = 2\eta\boldsymbol{\epsilon}$. Thereby, shear stress tensor ($\boldsymbol{\epsilon}$) is part of the decomposition of an unidirectional flow field. It resembles on the one hand side any stretching or squeezing of fluid by "extensional"

¹ For sake of completeness, it should be mentioned that viscous forces can also transfer energy irreversibly to internal energy. However, they are inversely proportional to the system's size, and hence omitted.

strain and on the other hand side “shear” strain which is responsible for skewing. [5]

$$\boldsymbol{\tau} = \boldsymbol{\tau}_{viscous} + \boldsymbol{\tau}_{pressure} = 2\eta\boldsymbol{\epsilon} - p\mathbf{I}_{3\times 3} \quad (1.6)$$

$$\nabla \cdot \boldsymbol{\tau}_{viscous} = \nabla \cdot 2\eta\boldsymbol{\epsilon} = \nabla \cdot \eta\nabla\mathbf{u} \stackrel{\text{only if } \eta \text{ uniform}}{=} \eta\nabla^2\mathbf{u} \quad (1.7)$$

$$\underbrace{\rho \frac{\partial \mathbf{u}}{\partial t}}_{\text{Transient}} + \underbrace{\rho \mathbf{u} \cdot \nabla \mathbf{u}}_{\text{Convection}} + \underbrace{-\nabla p}_{\text{Pressure}} + \underbrace{\eta \nabla^2 \mathbf{u}}_{\text{Viscous}} + \underbrace{\sum_i \mathbf{f}_i}_{\text{Body Forces}} = 0 \quad (1.8)$$

The divergence of $\boldsymbol{\tau}_{viscous}$, as used in the incompressible Cauchy momentum equation (Eq. 1.4), can then be simplified with Eq. 1.7 further by taking advantage of the anti-transpose symmetry of the flow field. If η is also uniform respectively isotropic across the channel, the divergence is completely independent of the scalar viscosity. Applying all assumptions to the Cauchy momentum equation (Eq. 1.4) yields as final result the Navier-Stokes-Equation (NSE). (Eq. 1.8)

However, the NSE has no analytic solution yet and can in consequence only solve defined boundary problems. The two most common boundary conditions herefore are the “no-penetration condition” ($\mathbf{u} \cdot \vec{n} = 0$) and the “no-slip condition” ($\mathbf{u}_t = \mathbf{u} - (\mathbf{u} \cdot \vec{n}) \vec{n} = 0$), which state that the normal and tangential components of fluid velocity are per definition zero at motionless, impermeable walls.

Besides these conditions, many problems arise due to turbulent flow and therefor transient effects. Mathematically, this can be avoided by simply neglecting the time-dependent term in the NSE. Also, it can be argued from a systematic point of view that, for viscosity-dominated flows, fluid moves in isoplanar “lamina”. In experimental observations, these laminar flows then proved to be stable to perturbations thus steady.

$$Re = \frac{\text{fluid density} \cdot \text{velocity} \cdot \text{size}}{\text{viscosity}} \quad (1.9)$$

In a first order approximation, the dimensionless Reynolds number (Re), which compares the inertia to viscous forces, allows a qualitative prognosis about the flow regime. (Eq. 1.9) If it results below a threshold of 2300, laminar flow can be assumed in Hagen-Poiseuille flows. This holds true for the utilized microfluidic with the dimensions 12 000 μm x 700 μm x 150 μm (l x w x h) and aequous buffer solutions, where the channel width considered as characteristic length l . Hence, several fluidic phenomena such

as deterministic pathlines as well as simplifications of the NSE can be exploited in the present system.

In the model case of a flow through a rectangular channel, no analytical solution of the NSE exists, but a Fourier Series expansion if the width is larger than height of a channel as shown in Bruus [6].² Equation 1.10 determines the magnitude of the flow field parallel to the pressure gradient in relation to the horizontal dimension y and vertical dimension z with respect to the channel dimensions height h and width w . An integration over the flow field in the channel cross section yields the flow rate (Q). (Eq. 1.11)

$$\mathbf{u}_x(y, z) = \frac{4h^2\Delta p}{\pi^3\eta l} \sum_{n, odd}^{\infty} \frac{1}{n^3} \left(1 - \frac{\cosh(n\pi\frac{y}{h})}{\cosh(n\pi\frac{w}{2h})} \right) \sin(n\pi\frac{z}{h}) \quad (1.10)$$

$$Q = \int_{-\frac{1}{2}w}^{\frac{1}{2}w} \int_0^h u_x(y, z) \, dz \, dy \approx \frac{h^3 w \Delta p}{12\eta l} \left(1 - \frac{h}{w} \right), \text{ for } h < w \quad (1.11)$$

1.1.3. Force Equilibrium of Microbeads

Although microfluidic systems mostly operate in a low inertia regimes as specified by low Re , the force equilibrium and subsequently the velocity of any particle in the fluid stream is influenced as it moves closer to the boundaries. Therefore, a short overview over all acting forces shall be given here.

² The equation 1.10 shows that height deviations can have prominent influence on a channel velocity simulation as it is proportional to h^2 . Further, the flow rate depends even on h^3 .

$$\mathbf{F}_{drag,wall} = -6\pi\eta r \bar{\mathbf{u}} K \quad (1.12)$$

$$K = \frac{4}{3} \sinh \alpha \sum_{n=0}^{\infty} \left(\frac{n(n+1)}{(2n-1)(2n+3)} \cdot A \right) \quad (1.13)$$

$$\alpha = \cosh^{-1} \frac{z}{r} \quad (1.14)$$

$$A = \left(\frac{2 \sinh((2n+1)\alpha) + (2n+1) \sinh 2\alpha}{(2 \sinh((n+0.5)\alpha))^2 - ((2n+1) \sinh \alpha)^2} - 1 \right) \quad (1.15)$$

$$K_{approx} = \frac{24}{Re} * \left(\frac{1 + \frac{2\eta_{fluid}}{3\eta_{particle}}}{1 + \frac{\eta_{fluid}}{\eta_{particle}}} \right) \quad (1.16)$$

$$v_z = \frac{3}{64} Re_s u_s = \frac{3}{64} \frac{\rho_{fluid} r u_s}{\eta} u_s, \left(\frac{\rho_{fluid} l_w u_s}{\eta} \right) \ll 1 \quad (1.17)$$

$$\mathbf{F}_{buoyancy} = -\frac{4}{3}\pi r^3 \rho_{fluid} g \quad (1.18)$$

$$\mathbf{F}_{gravity} = +\frac{4}{3}\pi r^3 \rho_{particle} g \quad (1.19)$$

$$\mathbf{F}_{shear} = \frac{81.2}{4} (\mathbf{u} - u_p) r^2 \sqrt{\frac{\rho_{fluid}}{\eta}} \nabla \mathbf{u} \quad (1.20)$$

$$\mathbf{F}_{magnus} = \frac{1}{8} \pi r^3 \rho_{fluid} (\mathbf{u} \times \boldsymbol{\Omega}) \quad (1.21)$$

$$\sum_i \mathbf{F} \stackrel{!}{=} 0 \quad (1.22)$$

$$\omega = \frac{0.025 r \mathbf{u}}{l^2 (1 - 0.6526 \frac{r}{l})}, \text{ for } \left(\frac{r}{l} \right)^2 \ll 1 \quad (1.23)$$

Stoke's Drag

The foremost force to move particles inside a microfluidic channel is Stoke's drag force (\mathbf{F}_{drag}). (Eq. 1.12) It originates in the viscous fluid moving past the sphere surface,

where a slip condition has to be applied. The fluid therefor has to displace its elements in front of the movement direction of a particle. [7] In the vertical dimension with a channel wall in the proximity, where no fluid can be displaced further, a correction factor was determined by that approximates drag in a perpendicular direction.(Eq. 1.13)[8]

A repusion velocity can then be defined by the Reynolds number calculated with the sedimentation velocity (u_s) if the particle center has a distance $l_w \ll 1$ from the wall. (1.17) [9] A phenomenological approximation of the correction factor yields equation 1.16, when viscosity dominates the difference. Adapted to an example, a spherical bubble inside a water flow feels only 67.4 % of the drag by the fluid.

zitat brenner

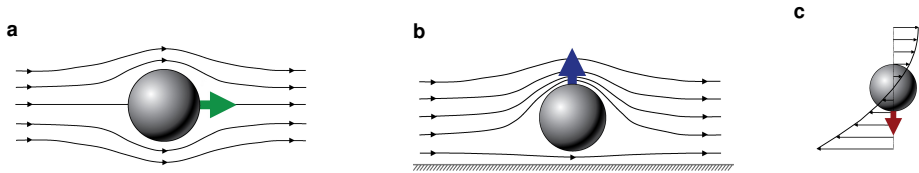


Figure 1: Particle Drag and Lift Behaviour

(a) Drag force on a particle caused by the displacement of fluid stream lines. (b) Wall-lift force: In a special case of drag, where no streamlines can be displaced, a pressure gradient forms in front of the sphere. This forces a motion directed perpendicularly from the wall. (c) Shear-induced force: The curvature of the flow profile exhibits a translation and rotation due to shear on the surface. [10]

$$Re_p = Re_{channel} \frac{r^2}{\frac{2wh}{w+h}} \quad (1.24)$$

Gravity and Buoyancy

On every mass in our environment acts gravity (\mathbf{F}_{grav}) to pull it along its gradient. In a medium however, it is balanced by the displacement of the same called buoyancy ($\mathbf{F}_{buoyancy}$) in the counter-direction. As a microparticle made from a co-polymer - especially when it is magnetic - has a significantly higher density than water, \mathbf{F}_{grav} (Eq. 1.19) outperforms $\mathbf{F}_{buoyancy}$ (Eq. 1.18), which in term causes a particle to sink to the channel floor.

Magnus Lift Force

The Magnus lift force (\mathbf{F}_{magnus}) is a rotation-induced variable as a result of the pressure difference induced by streamline asymmetry. [11]

Saffman Lift Force

When the rotation speed of a particle is much greater than the rate of shear for a freely rotating particle $\Omega > 12\nabla u$, “Saffman force” will begin to act. Depending on the interaction of slip velocity and shear, it will counteract any movement to the planar surface. Hence, at high gradients the center of rotation causes a shift to the maximum shear. Scaling with the rotation frequency (Ω), it will generally be at least one order of magnitude larger than Magnus force. Especially for electrically or magnetically actuated particles, Saffman force is more relevant in the case of non-neutrally buoyant spheres.[11]

Shear-induced Lift Force

This shear-induced lift force (\mathbf{F}_{shear}) particles to migrate toward walls until the wall lift force repels and balances it. In contrast, if the curvature of u is zero, it collapses to a

simple shear flow. Then the pressure will be higher on the far from the center pushing particles to the centerline of channel. As shown in 1c the magnitude of u in particle is much higher on the top side of particle than that on the bottom side, due to the parabolic nature of velocity profile. Similar to Saffman force, the dissymmetry of relative velocity causes a lower pressure on the wall side, generating a shear gradient lift force which is opposite to the Saffman force. [11]

Rotational Forces

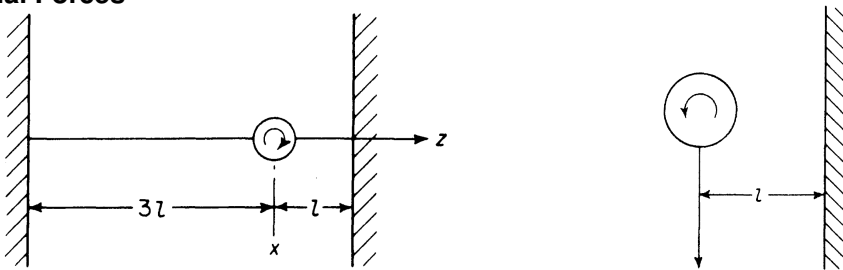


Figure 2: Particle Rotation Behaviour
tesrt

2.8 Deformability-induced lift force
Although solid rigid particles can be used as a simple model in the study of hydrodynamic behaviour of particles in a microchannel, the practical bio-particles such as cells and vesicles are not rigid but deformable. The deformability will induce additional lift forces on the particles. The deformability-induced lift force is perpendicular to the main streamline, and it is believed to be the effects of shape-change of particle and nonlinearities caused by the matching of velocities and stresses at the deformable particle interface

Deformability-induced lift force can be used to separate and enrich malaria-infected red blood cells (iRBCs) from normal healthy RBCs (hRBCs) for the diagnosis of malaria. The parasite releases proteins that trigger the cross-linking of the spectrin network in the iRBC's phospholipid bilayer membrane, thus increases the rigidity of the iRBCs. Normal hRBCs are more deformable than iRBCs, migrating towards the centre of the channel. Due to the massive hydrodynamic interactions and mechanical collisions between the RBCs in high haematocrit (Hct) blood, stiffer malaria iRBCs are displaced towards the sidewalls, and can be depleted and enriched by bifurcated outlets 48. In inertial microfluidics, Hur et al. 45 found that centre-directed deformability-induced lift force shifts inertial equilibrium positions a little closer to the channel centreline than that of rigid particles, Figure 2(c). By the combination of size and deformability, circulating

tumor cells (CTCs) with more deformability than the cells from the same organ, has been demonstrated to be separated and enriched from peripheral blood⁴⁵. Besides particle deformability, the shape of particles⁴⁹ and the properties of medium⁵⁰ also impact the inertial migration and equilibrium positions, which will not be discussed here. A summary of particle kinetics in inertial microfluidics is shown in Figure 3 Mach and Di Carlo⁵⁸ reported a massively parallelized microfluidic device that passively separates pathogenic bacteria from the diluted blood (Figure 5(b)). The device consists of 40 single straight micro-channels placed as a radial array. Each channel consists of three segments with different cross-sections, which uses a unique differential transit time by size-dependent inertial lift forces to obtain cell separation. The authors demonstrated that more

Gravity Electro-static interaction Magnetic Force Friction Interface-Forces Faraus linquist Protein interaction/ Avidity,Affinity

Rolling Motion of Beads

1.1.4.

1.2. Surface Chemistry

Introducing biological samples, such as peripheral whole blood and -plasma, into microsystems needs careful consideration of surface modification compared to buffered samples of adjusted pH containing cells or polymeric beads. Blood-material contact most often initiates surface-mediated reactions that lead to cell activation, blood clotting or biofilm formation. In order to minimize unspecific interactions on surfaces, most contact faces are passivated with chemically and biologically inert materials or even composed entirely from it. In any use case, where a surface has to be functionalized with biomolecules, the intrinsic inertness then requires specialized methods for permanent and reproducible adhesion.[12]

Molecules can be immobilized through various mechanisms on surfaces to achieve a biological or chemical functionality. The most simple is physisorption. Here, a biomolecule is bonded only by weak electrostatic, van-der-Waals or dipole-dipole interaction with a adsorption enthalpy below 50 kJ mol^{-1} . In contrast, this yields fast reaction rates, because no activation energy has to be overcome. Although a large number of molecules can be captured with this method, several drawbacks have been identified. [13], [14] For example, immobilized receptors can desorb or move inside the channel, which in turn reduces sensitivity or causes false-positive results. [15], [16]

Therefore, most functionalization approaches rely on chemisorption where molecules are covalently bound to a surface. Due to the higher activation energy barrier this bonding mechanism works slower in comparison to physisorption, though higher temperatures or catalysts can promote an equilibrium. One of the most well-known strategies to bring reproducible thin films on surfaces is the formation of self-assembled monolayers (SAMs) where a dense layer of single molecules with high internal order forms upon dipping into a surface-active substance. [17]

1.2.1. Surface Oxidation Methods

Modifying a surface with functional silanes, requires oxidized sites, for example –OH (hydroxyl) resp. Si–OH (silanol) groups. In order to increase the presence of those reactive groups on substrates, various activation methods such as piranha, a mixture from hydrogen peroxide (H_2O_2) and sulfuric acid (H_2SO_4), oxygen gas (O_2) - plasma treatment or an hydrofluoric acid (HF) dip can be chosen. [18]

Critical for any surface engineering is the internal structure and in consequence the binding energies of the surficial groups. The three mainly used substrates in this work, glass, poly(dimethyl siloxane) (PDMS) and silicon nitride (Si_3N_4), contain highly conserved, homogeneous surfaces and are mostly well characterized. The surface of glass exhibits already silanol groups intrinsically and consequentially demands only a removal of impurities. PDMS and Si_3N_4 however have different compositions as shown in Fig. ?? and 4 hence requiring a strong oxidation agents to completely exchange its interface. [19]–[21]

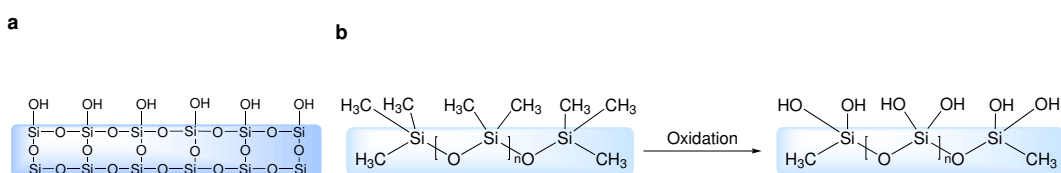
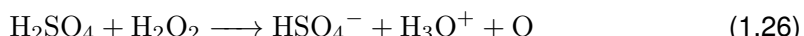
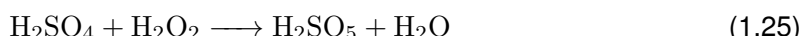


Figure 3: Different substrate surfaces: glass and PDMS

Surface groups and internal structure of quartz glass (a) and PDMS (b). After an oxidation step, the methyl groups are changed to hydroxyl.

Piranha Solution

Piranha is an oxidizer composed of H_2O_2 and H_2SO_4 , typically in volume ratios between 1:3 and 1:7. The effectiveness of piranha in removing organic residues and creating hydroxyl groups is induced by two distinct processes. In the first process, which is notably faster, hydrogen and oxygen are removed as units of water by the concentrated H_2SO_4 . (Reaction 1.25) This occurs due to the thermodynamically very favorable reaction with an enthalpy of -880 kJ mol^{-1} and produces Caro's acid (H_2SO_5), one of the strongest oxidants known. [22]



In another process the sulfuric acid boosts hydrogen peroxide from a mild oxidizer into the more aggressive atomic oxygen by the dehydration of H_2O_2 . (Reaction 1.26) These two dehydration processes in the mixture result on the one hand in a highly corrosive nature against organic materials, particularly against the difficult to remove carbon. On

the other hand, it is strongly acidic and oxidizing which in turn requires great care and substantial safety measures to prepare and use it harmlessly.

Hydrofluoric Acid

One of the used substrates in this work is Si_3N_4 as passivation layer above magnetic sensors as it has a significant better diffusion barrier against water or sodium ions and is chemically very inert. [23]

However, due to its complex crystal structure it is also difficult to modify by common chemicals and the exact surface composition still subject to scientific discussion. [24] Apart from cleaning the surface with piranha, few other modification methods have been reported, but only one suitable for the direct generation of hydroxyl groups.

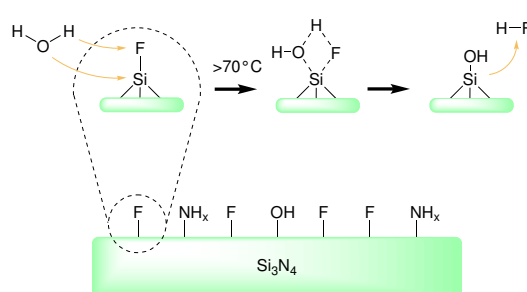


Figure 4: Proposed modification of Si_3N_4 with HF

There, as depicted in 4, the reaction $\text{Si}-\text{OH} + \text{HF} \rightleftharpoons \text{Si}-\text{F} + \text{H}_2\text{O}$ takes place reversibly due to the coincidence that $\text{Si}-\text{O}$ and $\text{O}-\text{H}$ as well as $\text{Si}-\text{F}$ and $\text{H}-\text{F}$ bonds have similar binding energies and hence the forward and reverse reactions a low activation energy. After Le Chatelier's principle, a depletion of HF in the bulk leads then to an increase in surficial hydroxyl groups. [25] In further works, it has been determined that an oxidation with a similar protocol based on aqueous HF yields a variable $\text{Si}-\text{O}-\text{Si}$ (siloxane) coverage with $37 \pm 17\%$ of a monolayer, which nevertheless can be used for stable, covalent attachment of silanes. Nominally the same surface coverages of silicon oxide and nitride surfaces could be achieved by ethoxy- and chlorosilanization. [26] As shown by [27], the subsequent surfaces exhibit beneficial biological properties and can be modified by further standard procedures.

Oxygen Plasma

Apart from wet chemistry methods, the exposure of a surface to oxygen plasma yields hydroxyl groups as well. In a plasma chamber, a low-pressure gas is irradiated by kHz to MHz waves to excite and ionize its atoms. In consequence, the UV-radiation emitted by the gas can photolyse typical organic bonds and remove surface contaminations. Additionally, reactive oxygen species such as O_2^+ , O_2^- , O_3 or O either oxidize the surface as well or bind dissociated components with low vapor pressure. During an evacuation in the process, these molecules are removed from the chamber intrinsically. [28]

1.2.2. Silane Chemistry

By the use of silane chemistry a surface is rendered organofunctional with alkoxy silane molecules. Since glass, silicon, alumina, titania, and quartz surfaces, as well as other metal oxide interfaces, are rich in hydroxyl groups, silanes are particularly useful for modifying these materials. [29]

The general formula for a silane coupling agent (Fig. 5) typically shows the two classes of functionality. X is a hydrolyzable group typically alkoxy, acyloxy, halogen or amine.

Following hydrolysis, a reactive silanol group is formed, which can condense with other silanol groups to form siloxane linkages. (Fig. 6) Stable condensation products are also formed with other oxides such as those of aluminum, zirconium, tin, titanium, and nickel. Less stable bonds are formed with oxides of boron, iron, and carbon, whereas alkali metal oxides and carbonates do not form stable bonds with siloxanes at all. The R group (Fig. 5) is a nonhydrolyzable organic radical that may possess a functionality that imparts desired characteristics. One of the more common silanes is (3-aminopropyl)triethoxysilane (APTES), where the X group consists of an $-\text{O}-\text{CH}_2-\text{CH}_3$ (ethoxy) group, the organic rest R is substituted by an $-\text{NH}_2$ (amine) and the 3 $-\text{CH}_2-$ (methylene) groups alter n to 3. [30]

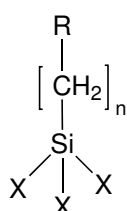


Figure 5: Trialkoxysilane
Structure of a typical trialkoxysilane, X: hydrolyzable group, R: non-hydrolyzable organic radical, n: methylene chain-length

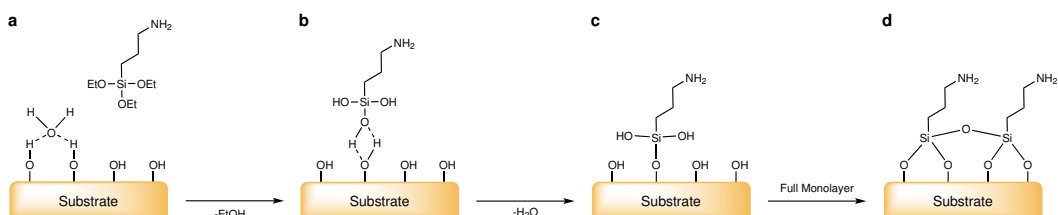


Figure 6: APTES Modification of an oxidized surface

a Before the condensation reaction, the oxidized surface forms hydrogen bonds with water molecules. The silane molecules are in the bulk solution. b The hydrolyzed silanol group adsorbs onto the surface and forms hydrogen bridges with it. c In a condensation reaction, under the loss of water, a covalent bond to the surface forms. d After the SAM assembly the surface is saturated with a covalent-bound, crosslinked silane film. [31]

The final result of reacting an organosilane with a substrate ranges from altering the wetting or adhesion characteristics of the substrate, utilizing the substrate to catalyze chemical transformation at the heterogeneous interface, ordering the interfacial region, and modifying its partition characteristics. Significantly, it includes the ability to effect a

covalent bond between organic and inorganic materials. Especially in optical or biological sensors, silane modifications open a broad range of applications.

However, the silanization reactions bear a few drawbacks which are often neglected. For instance, silane chemistry is strongly temperature and pH-dependent. [32], [33] Further, in a process to build SAMs out of APTES, the reaction has to be catalyzed by water. But already small changes in the water content cause dramatic deviations in layer thickness. [34] Additionally, silanes can crosslink to themselves through possible side reactions. (Fig. 6 D) [35]

1.2.3. Carbodiimide Crosslinker Chemistry

The in previous manner produced amine-terminated films by APTES form the basis of many reactions and open the possibility to various applications, such as the direct attachment of biofunctional molecules by carbodiimide crosslinking chemistry.[36] Here, $-COOH$ (carboxyl) groups are modified by 1-ethyl-3-(3-dimethylaminopropyl)carbodiimide (EDC) and N-hydroxysuccinimide (NHS) to form a stable secondary $R_1 - CONH - R_2$ (carboxamide) bond with any primary amine.

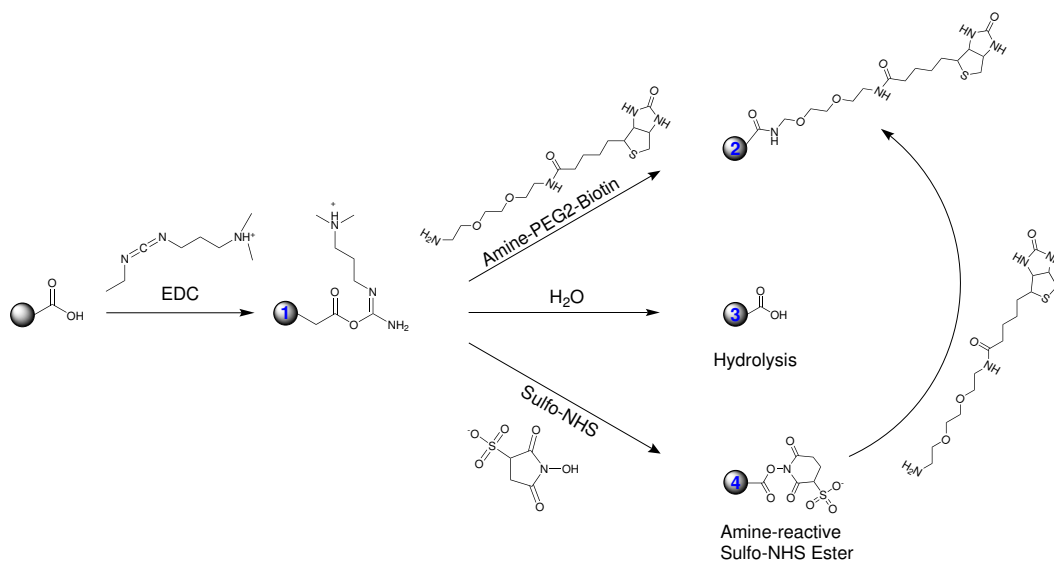


Figure 7: Carboxyl bead modification with EDC/NHS

The carboxyl groups bead are activated with EDC to an active O-acylisourea intermediate. This can then either be nucleophilically attacked by a primary amine of the amine-PEG₂-biotin reactant or - due to its instability - hydrolyzed back to a regenerated carboxyl surface. A present NHS-ester can also displace the O-acylisourea to form a considerably more stable intermediate which then itself reacts with any primary amine.

The general reaction mechanism is depicted in Fig. 7 for the example of a microbead surface, but it can equivalently be applied to any other modified surface or molecule. The initial carboxyl group is esterified by EDC to an active o-acylisourea intermediate and leaves rapidly upon nucleophilic attack of an amine with release of an iso-urea byproduct. A zero-length amide linkage is formed. (Fig. 7, 1->4) Sulphydryl and hydroxyl groups also will react with such active esters, but the products of such reactions, thioesters and esters, are relatively unstable compared to an carboxamide bond. (Fig. 7, 1)

However, this reactive complex is slow to react with amines and can hydrolyze in aqueous solutions, having a rate constant measured in seconds. If the target amine does not find the active carboxyl before it hydrolyzes (Fig. 7, 3), the desired coupling cannot occur. This is especially a problem when the target molecule is in low concentration compared to water, as in the case of protein molecules. Notwithstanding, forming a NHS ester intermediate from the reaction of the hydroxyl group on NHS with the EDC active-ester complex increases the resultant amide bond formation remarkably. (Fig. 7, 3->4) [37]

Another critical point in carbodiimide chemistry is the solubility of the compounds. EDC, NHS and N-hydroxysulfosuccinimide (sulfo-NHS) are soluble in aqueous and organic solvents. Nevertheless, activation with non-sulfonate NHS decreases water-solubility of the modified carboxylate molecule, while activation with sulfo-NHS preserves or increases its water-solubility by virtue of the charged sulfonate group. [38]

write!!!!

1.2.4. Microscopic Particle Surface Physics

1.2.5. The Biotin-Avidin-System

Until now, the interaction of the homotetrameric protein avidin and its ligand biotin forms one of the strongest known non-covalent bonds in biological systems characterized by a dissociation constant (K_d) in the range of 10^{-15} M.[39] First isolated from chicken egg white, it became a standard to use in biotechnology when researchers found a similar bacteria protein - streptavidin - in *Streptomyces* strains.[40] However, the charged glycoprotein avidin exhibits unspecific binding in some assays in comparison to streptavidin. Therefor, several companies developed deglycosylated forms of avidin with a neutral isoelectric points to minimize unspecificity. (NeutrAvidin, Extravidin, NeutraLite) In recent studies, a mutant streptavidin called "Traptavidin" exhibited an even 10 times dissociation rate.[41] As discovered in the early 1990s, biotin is bound inside a highly stable β -barrel structure, and stabilized by hydrogen bonds and van der Waals forces.[42] In a unique mechanism, a side group of biotin (valerate) binds to a neighboring monomer of streptavidin and therefor stabilizes the dimer complex intrinsically.[43], [44] From a thermodynamical point-of-view, the interaction of the vitamin and protein is described by a total free binding energy of 300 kJ mol^{-1} to 330 kJ mol^{-1} for a tetrameric protein. [44] All these aspects lead to a significant rupture force for the biotin-release of 250 pN .[45]

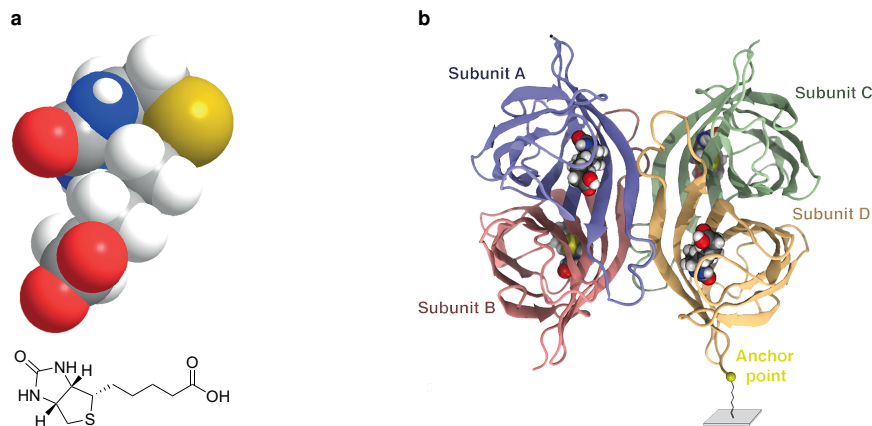


Figure 8: Functional Structures of Biotin and Streptavidin

(a) Biotin chemical structure, (b) Homotetrameric Streptavidin with the anchor point at one terminus.[46]

1.3. Magnetoresistive Sensing

Short intro in GMR Short intro over MRCyte

List of Abbreviations

Symbols

Q - flow rate.....
τ - surface stress tensor.....
$\tau_{pressure}$ - pressure stress tensor.....
$\tau_{viscous}$ - viscous stress tensor.....
ε - shear stress tensor
η - dynamic viscosity.....
$\mathbf{F}_{buoyancy}$ - buoyancy.....
\mathbf{F}_{drag} - Stoke's drag force
\mathbf{F}_{grav} - gravity
\mathbf{F}_{magnus} - Magnus lift force
\mathbf{F}_{shear} - shear-induced lift force
Ω - rotation frequency
Re - Reynolds number
μF - microfluidic
\mathbf{u} - flow field.....
\vec{n} - unit outward normal
ρ - density
$\sum_i \mathbf{F}_i$ - body forces
u_s - sedimentation velocity.....

A

AAF - artificial Anti-Ferromagnet.....
AcOH - acetic acid.....
AFM - Anti-Ferromagnetism.....
amine - $-\text{NH}_2$
APTES - (3-aminopropyl)triethoxysilane

C

carboxamide - $\text{R}_1 - \text{CONH} - \text{R}_2$
carboxyl - $- \text{COOH}$
CV - coefficient of variance

D

diH₂O - deionized water
DMSO - dimethyl sulfoxide.....

E

EDC - 1-ethyl-3-(3-dimethylaminopropyl)carbodiimide
ethoxy - –O–CH₂–CH₃
EtOH - ethanol.....

F

FM - Ferrimagnetism.....
FWHM - full width at half maximum.....

G

GMR - giant magneto resistance.....

H

H₂O₂ - hydrogen peroxide
H₂SO₅ - Caro's acid.....
H₂SO₄ - sulfuric acid.....
HCl - hydrochloric acid
HF - hydrofluoric acid.....
hydroxyl - –OH.....

I

IPA - isopropanol.....

K

K_d - dissociation constant.....

M

MACS - MACS running buffer.....
MeOH - methanol.....
MES - 2-(N-morpholino)ethanesulfonic acid.....
MEST - 2-(N-morpholino)ethanesulfonic acid (MES) buffer with Tween 20.....
methylene - –CH₂ –

MFI - median fluorescence intensity.....
MFLI - multi frequency lock-in

MNP - magnetic nanoparticle.....

N

N₂ - nitrogen gas.....
NFM - non-ferro-magnetic.....
NHS - N-hydroxysuccinimide.....
NSE - Navier-Stokes-Equation.....

O

O₂ - oxygen gas

P

PAA - Poly(acrylic) Acid.....
PBS - phosphate buffered saline

PBST - phosphate buffered saline (PBS) with Tween 20

PCB - printed circuit board.....
PDMS - poly(dimethyl siloxane).....
PM - Paramagnetism

S

SAM - self-assembled monolayer

Si₃N₄ - silicon nitride.....
silanol - Si-OH.....
siloxane - Si-O-Si

SMA - styrene maleic anhydride.....
SPM - superparamagnetism

sulfo-NHS - N-hydroxysulfosuccinimide

V

V_{pp} - peak-to-peak voltage.....
V_p - peak voltage.....

List of Figures

1 Particle Drag and Lift Behaviour	
(a) Drag force on a particle caused by the displacement of fluid stream lines. (b) Wall-lift force: In a special case of drag, where no streamlines can be displaced, a pressure gradient forms in front of the sphere. This forces a motion directed perpendicularly from the wall. (c) Shear-induced force: The curvature of the flow profile exhibits a translation and rotation due to shear on the surface. [10]	6
2 Particle Rotation Behaviour	
tesrt	7
3 Different substrate surfaces: glass and PDMS	
Surface groups and internal structure of quartz glass (a) and PDMS (b). After an oxidation step, the methyl groups are changed to hydroxyl.	11
4 Proposed modification of Si₃N₄ with HF	
.	13
5 Trialkoxysilane	
Structure of a typical trialkoxysilane, X: hydrolyzable group, R: non-hydrolyzable organic radical, n: methylene chain-length	14
6 APTES Modification of an oxidized surface	
a Before the condensation reaction, the oxidized surface forms hydrogen bonds with water molecules. The silane molecules are in the bulk solution. b The hydrolyzed silanol group adsorbs onto the surface and forms hydrogen bridges with it. c In a condensation reaction, under the loss of water, a covalent bond to the surface forms. d After the SAM assembly the surface is saturated with a covalent-bound, crosslinked silane film. [31]	14

7	Carboxyl bead modification with EDC/NHS	
	The carboxy groups bead are activated with EDC to an active O-acylisourea intermediate. This can then either be nucleophilicly attacked by a primary amine of the amine-PEG ₂ -biotin reactant or - due to its instability - hydrolyzed back to a regenerated carboxyl surface. A present NHS-ester can also displace the O-acylisourea to form a considerably more stable intermediate which then itself reacts with any primary amine.	15
8	Functional Structures of Biotin and Streptavidin	
	(a) Biotin chemical structure, (b) Homotetrameric Streptavidin with the anchor point at one terminus.[46]	17

List of Tables

Bibliography

- [1] M. Helou, "Magnetic flow cytometry," PhD Thesis, 2014.
- [2] M. Reisbeck, "Integration und quantitative analyse in der magnetischen durchflusszytometrie," Thesis, 2019.
- [3] J. Brenner, "Superparamagnetic nanoparticles in picoliter droplets for measurements with spin valves," Bachelor Thesis, 2018.
- [4] E. Räth, "Affinity-based cell rolling assays in magnetic flow cytometry," Thesis, 2020.
- [5] B. Kirby, *Micro- and Nanoscale Fluid Mechanics*. 2010, ISBN: 9780511760723. DOI: [10.1017/cbo9780511760723](https://doi.org/10.1017/cbo9780511760723).
- [6] H. Bruus, *Theoretical Microfluidics*. Technical University of Denmark: Oxford University Press, 2008, ISBN: 978–0–19–923508–7.
- [7] H. Brenner, "The slow motion of a sphere through a viscous fluid towards a plane surface," *Chemical Engineering Science*, vol. 16, no. 3-4, pp. 242–251, Dec. 1961. DOI: [10.1016/0009-2509\(61\)80035-3](https://doi.org/10.1016/0009-2509(61)80035-3).
- [8] D. Di Carlo, D. Irimia, R. G. Tompkins, and M. Toner, "Continuous inertial focusing, ordering, and separation of particles in microchannels," *Proceedings of the National Academy of Sciences*, vol. 104, no. 48, pp. 18 892–18 897, 2007, ISSN: 0027-8424. DOI: [10.1073/pnas.0704958104](https://doi.org/10.1073/pnas.0704958104).
- [9] L. Zeng, F. Najjar, S. Balachandar, and P. Fischer, "Forces on a finite-sized particle located close to a wall in a linear shear flow," *Physics of Fluids*, vol. 21, no. 3, p. 033 302, 2009, ISSN: 1070-6631. DOI: [10.1063/1.3082232](https://doi.org/10.1063/1.3082232).
- [10] J. M. Martel and M. Toner, "Inertial focusing in microfluidics," *Annual Review of Biomedical Engineering*, vol. 16, no. 1, pp. 371–396, 2014, PMID: 24905880. DOI: [10.1146/annurev-bioeng-121813-120704](https://doi.org/10.1146/annurev-bioeng-121813-120704).
- [11] J. Zhang, S. Yan, D. Yuan, G. Alici, N.-T. Nguyen, M. Ebrahimi Warkiani, and W. Li, "Fundamentals and applications of inertial microfluidics: A review," *Lab on a Chip*, vol. 16, no. 1, pp. 10–34, 2016, ISSN: 1473-0197. DOI: [10.1039/c5lc01159k](https://doi.org/10.1039/c5lc01159k).
- [12] S. K. Mitra and A. A. Saha, "Surface modification, methods," in *Encyclopedia of Microfluidics and Nanofluidics*, Springer US, 2014, pp. 1–9. DOI: [10.1007/978-3-642-27758-0_1503-2](https://doi.org/10.1007/978-3-642-27758-0_1503-2).

- [13] W. Putzbach and N. Ronkainen, "Immobilization techniques in the fabrication of nanomaterial-based electrochemical biosensors: A review," *Sensors*, vol. 13, no. 4, pp. 4811–4840, 2013, ISSN: 1424-8220. DOI: 10.3390/s130404811.
- [14] R. Funari, B. Della Ventura, C. Altucci, A. Offenhäusser, D. Mayer, and R. Velotta, "Single molecule characterization of uv-activated antibodies on gold by atomic force microscopy," *Langmuir*, vol. 32, no. 32, pp. 8084–8091, 2016, ISSN: 0743-7463. DOI: 10.1021/acs.langmuir.6b02218.
- [15] A. Ymeti, J. Kanger, J. Greve, G. Besselink, P. Lambeck, R. Wijn, and R. Heideman, "Integration of microfluidics with a four-channel integrated optical young interferometer immunosensor," *Biosensors and Bioelectronics*, vol. 20, no. 7, pp. 1417–1421, 2005, ISSN: 0956-5663. DOI: <https://doi.org/10.1016/j.bios.2004.04.015>.
- [16] M.-J. Bañuls, R. Puchades, and Á. Maquieira, "Chemical surface modifications for the development of silicon-based label-free integrated optical (io) biosensors: A review," *Analytica Chimica Acta*, vol. 777, pp. 1–16, 2013, ISSN: 0003-2670. DOI: 10.1016/j.aca.2013.01.025.
- [17] N. Lange, "Selective chemical modification of silicon nitride surfaces for novel biosensor application," Thesis, 2017. DOI: <http://dx.doi.org/10.17169/refubium-11275>.
- [18] M. Brunet, D. Aureau, P. Chantraine, F. Guillemot, A. Etcheberry, A. C. Gouget-Laemmel, and F. Ozanam, "Etching and chemical control of the silicon nitride surface," *ACS Applied Materials & Interfaces*, vol. 9, no. 3, pp. 3075–3084, 2017, ISSN: 1944-8244. DOI: 10.1021/acsami.6b12880.
- [19] K. Sekine, Y. Saito, M. Hirayama, and T. Ohmi, "Highly robust ultrathin silicon nitride films grown at low-temperature by microwave-excitation high-density plasma for giga scale integration," *IEEE Transactions on Electron Devices*, vol. 47, no. 7, pp. 1370–1374, 2000, ISSN: 0018-9383. DOI: 10.1109/16.848279.
- [20] M. K. Chaudhury and G. M. Whitesides, "Correlation between surface free energy and surface constitution," *Science*, vol. 255, no. 5049, pp. 1230–1232, 1992, ISSN: 0036-8075. DOI: 10.1126/science.255.5049.1230.
- [21] H. Hillborg, J. Ankner, U. Gedde, G. Smith, H. Yasuda, and K. Wikström, "Crosslinked polydimethylsiloxane exposed to oxygen plasma studied by neutron reflectometry and other surface specific techniques," *Polymer*, vol. 41, no. 18, pp. 6851–

- 6863, 2000, ISSN: 0032-3861. DOI: [https://doi.org/10.1016/S0032-3861\(00\)00039-2](https://doi.org/10.1016/S0032-3861(00)00039-2).
- [22] A. N. Ermakov, I. K. Larin, Y. N. Kozlov, and A. P. Purmal', "The thermodynamic characteristics of hydrogen peroxide in h₂so₄-h₂o solutions," *Russian Journal of Physical Chemistry A*, vol. 80, no. 12, pp. 1895–1901, 2006, ISSN: 0036-0244. DOI: 10.1134/s0036024406120041.
- [23] M. Yashima, Y. Ando, and Y. Tabira, "Crystal structure and electron density of α-silicon nitride: experimental and theoretical evidence for the covalent bonding and charge transfer," *The Journal of Physical Chemistry B*, vol. 111, no. 14, pp. 3609–3613, 2007, ISSN: 1520-6106. DOI: 10.1021/jp0678507.
- [24] M. Brunet, D. Aureau, P. Chantraine, F. Guillemot, A. Etcheberry, A. C. Gouget-Laemmel, and F. Ozanam, "Etching and chemical control of the silicon nitride surface," *ACS Applied Materials & Interfaces*, vol. 9, no. 3, pp. 3075–3084, 2017, ISSN: 1944-8244. DOI: 10.1021/acsami.6b12880.
- [25] D. J. Michalak, S. R. Amy, D. Aureau, M. Dai, A. Estève, and Y. J. Chabal, "Nanopatterning si(111) surfaces as a selective surface-chemistry route," *Nature Materials*, vol. 9, no. 3, pp. 266–271, 2010, ISSN: 1476-1122. DOI: 10.1038/nmat2611.
- [26] L. H. Liu, D. J. Michalak, T. P. Chopra, S. P. Pujari, W. Cabrera, D. Dick, J. F. Veyan, R. Hourani, M. D. Halls, H. Zuilhof, and Y. J. Chabal, "Surface etching, chemical modification and characterization of silicon nitride and silicon oxide—selective functionalization of si₃n₄ and sio₂," *J Phys Condens Matter*, vol. 28, no. 9, p. 094014, 2016, ISSN: 1361-648X (Electronic) 0953-8984 (Linking). DOI: 10.1088/0953-8984/28/9/094014.
- [27] J. Gustavsson, G. Altankov, A. Errachid, J. Samitier, J. A. Planell, and E. Engel, "Surface modifications of silicon nitride for cellular biosensor applications," *Journal of Materials Science: Materials in Medicine*, vol. 19, no. 4, pp. 1839–1850, 2008, ISSN: 0957-4530. DOI: 10.1007/s10856-008-3384-7.
- [28] A. Pizzi and K. Mittal, *Handbook of Adhesive Technology, Revised and Expanded*. Taylor and Francis, 2003, ISBN: 9780203912225.
- [29] B. Seed, "Silanizing glassware," *Current Protocols in Cell Biology*, vol. 8, no. 1, A.3E.1–A.3E.2, 2000, ISSN: 1934-2500. DOI: 10.1002/0471143030.cba03es08.
- [30] GELEST, *Silane coupling agents*, Catalog, 2014.

- [31] H. Khanjanzadeh, R. Behrooz, N. Bahramifar, S. Pinkl, and W. Gindl-Altmutter, “Application of surface chemical functionalized cellulose nanocrystals to improve the performance of uf adhesives used in wood based composites - mdf type,” *Carbohydrate Polymers*, vol. 206, pp. 11–20, 2019, ISSN: 0144-8617. DOI: <https://doi.org/10.1016/j.carbpol.2018.10.115>.
- [32] N. B. Arnfinnisdottir, C. A. Chapman, R. C. Bailey, A. Aksnes, and B. T. Stokke, “Impact of silanization parameters and antibody immobilization strategy on binding capacity of photonic ring resonators,” *Sensors*, vol. 20, no. 11, 2020, ISSN: 1424-8220. DOI: 10.3390/s20113163.
- [33] R. M. Pasternack, S. Rivillon Amy, and Y. J. Chabal, “Attachment of 3-(aminopropyl)triethoxysilane on silicon oxide surfaces: Dependence on solution temperature,” *Langmuir*, vol. 24, no. 22, pp. 12 963–12 971, 2008, ISSN: 0743-7463. DOI: 10.1021/la8024827.
- [34] M. J. Banuls, V. Gonzalez-Pedro, C. A. Barrios, R. Puchades, and A. Maquieira, “Selective chemical modification of silicon nitride/silicon oxide nanostructures to develop label-free biosensors,” *Biosens Bioelectron*, vol. 25, no. 6, pp. 1460–6, 2010, ISSN: 1873-4235 (Electronic) 0956-5663 (Linking). DOI: 10.1016/j.bios.2009.10.048.
- [35] D. W. Sindorf and G. E. Maciel, “Solid-state nmr studies of the reactions of silica surfaces with polyfunctional chloromethylsilanes and ethoxymethylsilanes,” *Journal of the American Chemical Society*, vol. 105, no. 12, pp. 3767–3776, 1983, ISSN: 0002-7863. DOI: 10.1021/ja00350a003.
- [36] *Bioconjugate Techniques*. Elsevier, 2013. DOI: 10.1016/c2009-0-64240-9.
- [37] D. Hoare and D. Koshland, “A method for the quantitative modification and estimation of carboxylic acid groups in proteins,” *Journal of Biological Chemistry*, vol. 242, no. 10, pp. 2447–2453, May 1967. DOI: 10.1016/s0021-9258(18)95981-8.
- [38] T. Scientific, *User guide: Nhs and sulfo-nhs*, 2021.
- [39] D. W. Woolley and L. G. Longsworth, “Isolation of an antibiotic factor from egg white.,” *Journal of Biological Chemistry*, vol. 142, pp. 285–290, 1942.
- [40] T. Sano and C. R. Cantor, “Expression of a cloned streptavidin gene in escherichia coli.,” *Proceedings of the National Academy of Sciences*, vol. 87, no. 1, pp. 142–146, 1990, ISSN: 0027-8424. DOI: 10.1073/pnas.87.1.142.
- [41] C. E. Chivers, E. Crozat, C. Chu, V. T. Moy, D. J. Sherratt, and M. Howarth, “A streptavidin variant with slower biotin dissociation and increased mechanosta-

- bility," *Nature Methods*, vol. 7, no. 5, pp. 391–393, 2010, ISSN: 1548-7091. DOI: 10.1038/nmeth.1450.
- [42] P. Weber, D. Ohlendorf, J. Wendoloski, and F. Salemme, "Structural origins of high-affinity biotin binding to streptavidin," *Science*, vol. 243, no. 4887, pp. 85–88, 1989, ISSN: 0036-8075. DOI: 10.1126/science.2911722.
- [43] B. Miroux and J. E. Walker, "Over-production of proteins in escherichia coli: Mutant hosts that allow synthesis of some membrane proteins and globular proteins at high levels," *Journal of Molecular Biology*, vol. 260, no. 3, pp. 289–298, 1996, ISSN: 0022-2836. DOI: 10.1006/jmbi.1996.0399.
- [44] S. Miyamoto and P. A. Kollman, "Absolute and relative binding free energy calculations of the interaction of biotin and its analogs with streptavidin using molecular dynamics/free energy perturbation approaches," *Proteins: Structure, Function, and Bioinformatics*, vol. 16, no. 3, pp. 226–245, 1993, ISSN: 0887-3585. DOI: 10.1002/prot.340160303.
- [45] H., B. Heymann, and P. Tavan, "Ligand binding: Molecular mechanics calculation of the streptavidin-biotin rupture force," *Science*, vol. 271, no. 5251, pp. 997–999, 1996, ISSN: 0036-8075. DOI: 10.1126/science.271.5251.997.
- [46] S. M. Sedlak, L. C. Schendel, H. E. Gaub, and R. C. Bernardi, "Streptavidin/biotin: Tethering geometry defines unbinding mechanics," *Science Advances*, vol. 6, no. 13, 2020. DOI: 10.1126/sciadv.aay5999.
- [47] R. Hicsanmaz, "Setup and assessment of laser lithography for the fabrication and integration of biosensor and microfluidic devices," Technical University Munich, 2020.
- [48] W. J. Dressick, C. S. Dulcey, J. H. Georger, G. S. Calabrese, and J. M. Calvert, "Covalent binding of pd catalysts to ligating self-assembled monolayer films for selective electroless metal deposition," *Journal of the Electrochemical Society*, vol. 141, no. 1, pp. 210–220, 1994, ISSN: 0013-4651. DOI: 10.1149/1.2054686.
- [49] K. C. Andree, A. M. Barradas, A. T. Nguyen, A. Mentink, I. Stojanovic, J. Bagerman, J. van Dalum, C. J. van Rijn, and L. W. Terstappen, "Capture of tumor cells on anti-epcam-functionalized poly(acrylic acid)-coated surfaces," *ACS Appl Mater Interfaces*, vol. 8, no. 23, pp. 14349–56, 2016, ISSN: 1944-8252 (Electronic) 1944-8244 (Linking). DOI: 10.1021/acsami.6b01241.
- [50] A. Stalder, G. Kulik, D. Sage, L. Barbieri, and P. Hoffmann, "A snake-based approach to accurate determination of both contact points and contact angles,"

Colloids And Surfaces A: Physicochemical And Engineering Aspects, vol. 286, no. 1-3, pp. 92–103, Sep. 2006.

- [51] J. Schindelin, I. Arganda-Carreras, E. Frise, V. Kaynig, M. Longair, T. Pietzsch, S. Preibisch, C. Rueden, S. Saalfeld, B. Schmid, and et al., “Fiji: An open-source platform for biological-image analysis,” *Nature Methods*, vol. 9, no. 7, pp. 676–682, 2012, ISSN: 1548-7091. DOI: 10.1038/nmeth.2019.
- [52] “Syringe pumps.” (2021), [Online]. Available: <https://www.fluigent.com/resources/microfluidic-expertise/what-is-microfluidic/system-comparison-for-microfluidic-applications/>.
- [53] A. P. Guimarães, *Principles of Nanomagnetism*. Springer International Publishing, 2017. DOI: 10.1007/978-3-319-59409-5.
- [54] micromod Partikeltechnologie GmbH, *Technical data sheet - nanomag®-d-spio 50nm*, 2018.
- [55] M. J. Owen and P. J. Smith, “Plasma treatment of polydimethylsiloxane,” *Journal of Adhesion Science and Technology*, vol. 8, no. 10, pp. 1063–1075, 1994. DOI: 10.1163/156856194X00942.
- [56] C.-G. Stefanita, *Magnetism*. Springer Berlin Heidelberg, 2012. DOI: 10.1007/978-3-642-22977-0.
- [57] K. H. J. Buschow and F. R. de Boer, *Physics of Magnetism and Magnetic Materials*. Springer US, 2003. DOI: 10.1007/b100503.
- [58] G. C. Papaefthymiou, “Nanoparticle magnetism,” *Nano Today*, vol. 4, no. 5, pp. 438–447, Oct. 2009. DOI: 10.1016/j.nantod.2009.08.006.
- [59] P. Gravesen, J. Branebjerg, and O. S. Jensen, “Microfluidics-a review,” *Journal of Micromechanics and Microengineering*, vol. 3, no. 4, pp. 168–182, Dec. 1993. DOI: 10.1088/0960-1317/3/4/002.
- [60] K. C. Andree, A. M. Barradas, A. T. Nguyen, A. Mentink, I. Stojanovic, J. Baggerman, J. van Dalum, C. J. van Rijn, and L. W. Terstappen, “Capture of tumor cells on anti-epcam-functionalized poly(acrylic acid)-coated surfaces,” *ACS Applied Materials Interfaces*, vol. 8, no. 23, pp. 14349–56, 2016, ISSN: 1944-8252 (Electronic) 1944-8244 (Linking). DOI: 10.1021/acsami.6b01241.
- [61] G. Antonacci, J. Goyvaerts, H. Zhao, B. Baumgartner, B. Lendl, and R. Baets, “Ultra-sensitive refractive index gas sensor with functionalized silicon nitride photonic circuits,” *APL Photonics*, vol. 5, no. 8, 2020, ISSN: 2378-0967. DOI: 10.1063/5.0013577.

- [62] A. Arafat, M. Giesbers, M. Rosso, E. J. R. Sudhölter, K. Schroën, R. G. White, L. Yang, M. R. Linford, and H. Zuilhof, “Covalent biofunctionalization of silicon nitride surfaces,” *Langmuir*, vol. 23, no. 11, pp. 6233–6244, 2007, ISSN: 0743-7463 1520-5827. DOI: 10.1021/la7007045.
- [63] A. Arafat, K. Schroen, L. C. de Smet, E. J. Sudholter, and H. Zuilhof, “Tailor-made functionalization of silicon nitride surfaces,” *J Am Chem Soc*, vol. 126, no. 28, pp. 8600–1, 2004, ISSN: 0002-7863 (Print) 0002-7863 (Linking). DOI: 10.1021/ja0483746.
- [64] B. Baur, G. Steinhoff, J. Hernando, O. Purrucker, M. Tanaka, B. Nickel, M. Stutzmann, and M. Eickhoff, “Chemical functionalization of gan and aln surfaces,” *Applied Physics Letters*, vol. 87, no. 26, p. 263901, 2005, ISSN: 0003-6951. DOI: 10.1063/1.2150280.
- [65] J. Diao, D. Ren, J. R. Engstrom, and K. H. Lee, “A surface modification strategy on silicon nitride for developing biosensors,” *Anal Biochem*, vol. 343, no. 2, pp. 322–8, 2005, ISSN: 0003-2697 (Print) 0003-2697 (Linking). DOI: 10.1016/j.ab.2005.05.010.
- [66] T. Ghonge, H. Ceylan Koydemir, E. Valera, J. Berger, C. Garcia, N. Nawar, J. Tiao, G. L. Damhorst, A. Ganguli, U. Hassan, A. Ozcan, and R. Bashir, “Smartphone-imaged microfluidic biochip for measuring cd64 expression from whole blood,” *Analyst*, vol. 144, no. 13, pp. 3925–3935, 2019, ISSN: 1364-5528 (Electronic) 0003-2654 (Linking). DOI: 10.1039/c9an00532c.
- [67] M. Hofstetter, J. Howgate, M. Schmid, S. Schoell, M. Sachsenhauser, D. Adigüzel, M. Stutzmann, I. D. Sharp, and S. Thalhammer, “In vitro bio-functionality of gallium nitride sensors for radiation biophysics,” *Biochemical and Biophysical Research Communications*, vol. 424, no. 2, pp. 348–353, 2012, ISSN: 0006-291X. DOI: 10.1016/j.bbrc.2012.06.142.
- [68] D. Kim and A. E. Herr, “Protein immobilization techniques for microfluidic assays,” *Biomicrofluidics*, vol. 7, no. 4, p. 41501, 2013, ISSN: 1932-1058 (Print) 1932-1058 (Linking). DOI: 10.1063/1.4816934.
- [69] J. Klug, L. A. Pérez, E. A. Coronado, and G. I. Lacconi, “Chemical and electrochemical oxidation of silicon surfaces functionalized with aptes: The role of surface roughness in the aunps anchoring kinetics,” *The Journal of Physical Chemistry C*, vol. 117, no. 21, pp. 11317–11327, 2013, ISSN: 1932-7447 1932-7455. DOI: 10.1021/jp212613f.

- [70] N. Lange, P. M. Dietrich, A. Lippitz, N. Kulak, and W. E. S. Unger, “New azidation methods for the functionalization of silicon nitride and application in copper-catalyzed azide-alkyne cycloaddition (cuaac),” *Surface and Interface Analysis*, vol. 48, no. 7, pp. 621–625, 2016, ISSN: 01422421. DOI: 10.1002/sia.5950.
- [71] A. P. Le Brun, S. A. Holt, D. S. Shah, C. F. Majkrzak, and J. H. Lakey, “The structural orientation of antibody layers bound to engineered biosensor surfaces,” *Biomaterials*, vol. 32, no. 12, pp. 3303–11, 2011, ISSN: 1878-5905 (Electronic) 0142-9612 (Linking). DOI: 10.1016/j.biomaterials.2011.01.026.
- [72] M. E. Marques, A. A. P. Mansur, and H. S. Mansur, “Chemical functionalization of surfaces for building three-dimensional engineered biosensors,” *Applied Surface Science*, vol. 275, pp. 347–360, 2013, ISSN: 01694332. DOI: 10.1016/j.apsusc.2012.12.099.
- [73] A. Psarouli, A. Bourkoula, P. Petrou, K. Misiakos, N. Chaniotakis, and S. Kakabakos, “Covalent binding vs. adsorption of biomolecules on silicon nitride planar waveguides,” *Procedia Engineering*, vol. 25, pp. 350–353, 2011, ISSN: 18777058. DOI: 10.1016/j.proeng.2011.12.086.
- [74] M. Rosso, *Modification of Silicon Nitride and Silicon Carbide Surfaces for Food and Biosensor Applications*. 2009, ISBN: 978-90-8585-379-4.
- [75] P. Saengdee, C. Promptmas, S. Thanapitak, A. Srisuwan, A. Pankiew, N. Thornyanadacha, W. Chaisriratanakul, E. Chaowicharat, and W. Jeamsaksiri, “Optimization of 3-aminopropyltriethoxysilane functionalization on silicon nitride surface for biomolecule immobilization,” *Talanta*, vol. 207, p. 120 305, 2020, ISSN: 1873-3573 (Electronic) 0039-9140 (Linking). DOI: 10.1016/j.talanta.2019.120305.
- [76] S. Tan, L. Wang, J. Yu, C. Hou, R. Jiang, Y. Li, and Q. Liu, “Dna-functionalized silicon nitride nanopores for sequence-specific recognition of dna biosensor,” *Nanoscale Research Letters*, vol. 10, no. 1, 2015, ISSN: 1556-276X. DOI: 10.1186/s11671-015-0909-0.
- [77] T. D. To, A. T. Nguyen, K. N. T. Phan, A. T. T. Truong, T. C. D. Doan, and C. M. Dang, “Modification of silicon nitride surfaces with gopes and aptes for antibody immobilization: Computational and experimental studies,” *Advances in Natural Sciences: Nanoscience and Nanotechnology*, vol. 6, no. 4, 2015, ISSN: 2043-6262. DOI: 10.1088/2043-6262/6/4/045006.
- [78] P. Vermette, T. Gengenbach, U. Divisekera, P. A. Kambouris, H. J. Griesser, and L. Meagher, “Immobilization and surface characterization of neutravidin biotin-

- binding protein on different hydrogel interlayers," *Journal of Colloid and Interface Science*, vol. 259, no. 1, pp. 13–26, 2003, ISSN: 00219797. DOI: 10 . 1016 / s0021-9797(02)00185-6.
- [79] C. R. Vistas, A. C. P. Águas, and G. N. M. Ferreira, "Silanization of glass chips—a factorial approach for optimization," *Applied Surface Science*, vol. 286, pp. 314–318, 2013, ISSN: 01694332. DOI: 10 . 1016/j.apsusc . 2013 . 09 . 077.
- [80] C. Wang, Q. Yan, H.-B. Liu, X.-H. Zhou, and S.-J. Xiao, "Different edc/nhs activation mechanisms between paa and pmaa brushes and the following amidation reactions," *Langmuir*, vol. 27, no. 19, pp. 12 058–12 068, 2011, ISSN: 0743-7463 1520-5827. DOI: 10 . 1021/la202267p.
- [81] M. Yüce and H. Kurt, "How to make nanobiosensors: Surface modification and characterisation of nanomaterials for biosensing applications," *RSC Adv.*, vol. 7, no. 78, pp. 49 386–49 403, 2017, ISSN: 2046-2069. DOI: 10 . 1039/c7ra10479k.
- [82] K. AbuZineh, L. I. Joudeh, B. Al Alwan, S. M. Hamdan, J. S. Merzaban, and S. Habuchi, "Microfluidics-based super-resolution microscopy enables nanoscopic characterization of blood stem cell rolling," *Sci Adv*, vol. 4, no. 7, eaat5304, 2018, ISSN: 2375-2548 (Electronic) 2375-2548 (Linking). DOI: 10 . 1126 / sciadv . aat5304.
- [83] B. Alberts, A. Johnson, J. Lewis, D. Morgan, M. Raff, K. Roberts, and P. Walter, *Molecular Biology of the Cell*, ISBN: 0815345240.
- [84] K.-C. Chang and D. A. Hammer, "The forward rate of binding of surface-tethered reactants: Effect of relative motion between two surfaces," *Biophysical Journal*, vol. 76, no. 3, pp. 1280–1292, 1999, ISSN: 0006-3495. DOI: 10 . 1016 / s0006 - 3495 (99)77291-7.
- [85] R. Cheng, T. Zhu, and L. Mao, "Three-dimensional and analytical modeling of microfluidic particle transport in magnetic fluids," *Microfluidics and Nanofluidics*, vol. 16, no. 6, pp. 1143–1154, 2013, ISSN: 1613-4982 1613-4990. DOI: 10 . 1007 / s10404-013-1280-z.
- [86] S. Choi, O. Levy, M. B. Coelho, J. M. Cabral, J. M. Karp, and R. Karnik, "A cell rolling cytometer reveals the correlation between mesenchymal stem cell dynamic adhesion and differentiation state," *Lab Chip*, vol. 14, no. 1, pp. 161–6, 2014, ISSN: 1473-0189 (Electronic) 1473-0189 (Linking). DOI: 10 . 1039 / c3lc50923k.

- [87] M. Dembo, D. C. Torney, K. Saxman, and D. Hammer, “The reaction-limited kinetics of membrane-to-surface adhesion and detachment,” *Proceedings of the Royal Society of London. Series B. Biological Sciences*, vol. 234, no. 1274, pp. 55–83, 1997, ISSN: 0080-4649 2053-9193. DOI: 10.1098/rspb.1988.0038.
- [88] S. J. DeNardo, G. L. DeNardo, A. Natarajan, L. A. Miers, A. R. Foreman, C. Gruettner, G. N. Adamson, and R. Ivkov, “Thermal dosimetry predictive of efficacy of 111in-chl6 nanoparticle amf-induced thermoablative therapy for human breast cancer in mice,” *J Nucl Med*, vol. 48, no. 3, pp. 437–44, 2007, ISSN: 0161-5505 (Print) 0161-5505 (Linking).
- [89] B. Doffek, “Magnetic flow cytometry for thrombocyte analysis,” Thesis, 2015.
- [90] C. Dong and X. X. Lei, “Biomechanics of cell rolling: Shear flow, cell-surface adhesion, and cell deformability,” *Journal of Biomechanics*, vol. 33, no. 1, pp. 35–43, 2000, ISSN: 00219290. DOI: 10.1016/s0021-9290(99)00174-8.
- [91] M. Ermis, E. Antmen, and V. Hasirci, “Micro and nanofabrication methods to control cell-substrate interactions and cell behavior: A review from the tissue engineering perspective,” *Bioact Mater*, vol. 3, no. 3, pp. 355–369, 2018, ISSN: 2452-199X (Electronic) 2452-199X (Linking). DOI: 10.1016/j.bioactmat.2018.05.005.
- [92] M. A. M. Gijs, “Magnetic bead handling on-chip: New opportunities for analytical applications,” *Microfluidics and Nanofluidics*, 2004, ISSN: 1613-4982 1613-4990. DOI: 10.1007/s10404-004-0010-y.
- [93] C. Grütter, K. Müller, J. Teller, F. Westphal, A. Foreman, and R. Ivkov, “Synthesis and antibody conjugation of magnetic nanoparticles with improved specific power absorption rates for alternating magnetic field cancer therapy,” *Journal of Magnetism and Magnetic Materials*, vol. 311, no. 1, pp. 181–186, 2007, ISSN: 03048853. DOI: 10.1016/j.jmmm.2006.10.1151.
- [94] H. Happel John; Brenner, *Low Reynolds number hydrodynamics*, ser. Mechanics of fluids and transport processes. 1981, ISBN: 978-94-009-8352-6. DOI: 10.1007/978-94-009-8352-6.
- [95] U. Hassan, T. Ghonge, J. Reddy B., M. Patel, M. Rappleye, I. Taneja, A. Tanna, R. Healey, N. Manusry, Z. Price, T. Jensen, J. Berger, A. Hasnain, E. Flaugher, S. Liu, B. Davis, J. Kumar, K. White, and R. Bashir, “A point-of-care microfluidic biochip for quantification of cd64 expression from whole blood for sepsis strat-

- ification," *Nat Commun*, vol. 8, p. 15949, 2017, ISSN: 2041-1723 (Electronic) 2041-1723 (Linking). DOI: 10.1038/ncomms15949.
- [96] M. Hejazian, W. Li, and N. T. Nguyen, "Lab on a chip for continuous-flow magnetic cell separation," *Lab Chip*, vol. 15, no. 4, pp. 959–70, 2015, ISSN: 1473-0189 (Electronic) 1473-0189 (Linking). DOI: 10.1039/c4lc01422g.
- [97] M. Helou, M. Reisbeck, S. F. Tedde, L. Richter, L. Bär, J. J. Bosch, R. H. Stauber, E. Quandt, and O. Hayden, "Time-of-flight magnetic flow cytometry in whole blood with integrated sample preparation," *Lab on a Chip*, vol. 13, no. 6, 2013, ISSN: 1473-0197 1473-0189. DOI: 10.1039/c3lc41310a.
- [98] Y.-C. Hsiao, R. Khojah, X. Li, A. Kundu, C. Chen, D. B. Gopman, A. C. Chavez, T. Lee, Z. Xiao, A. E. Sepulveda, R. N. Candler, G. P. Carman, D. Di Carlo, and C. S. Lynch, "Capturing magnetic bead-based arrays using perpendicular magnetic anisotropy," *Applied Physics Letters*, vol. 115, no. 8, 2019, ISSN: 0003-6951 1077-3118. DOI: 10.1063/1.5085354.
- [99] J. J. S. Jr, "A method of calibrating helmholtz coils for the measurement of permanent magnets,"
- [100] G. Kokkinis, S. Cardoso, F. Keplinger, and I. Giouroudi, "Microfluidic platform with integrated gmr sensors for quantification of cancer cells," *Sensors and Actuators B: Chemical*, vol. 241, pp. 438–445, 2017, ISSN: 09254005. DOI: 10.1016/j.snb.2016.09.189.
- [101] J. M. Koo and C. Kleinstreuer, "Liquid flow in microchannels: Experimental observations and computational analyses of microfluidics effects," *Journal of Micromechanics and Microengineering*, vol. 13, no. 5, pp. 568–579, 2003, ISSN: 0960-1317. DOI: PiS0960-1317(03)57671-9Doi10.1088/0960-1317/13/5/307.
- [102] H. G. Kye, B. S. Park, J. M. Lee, M. G. Song, H. G. Song, C. D. Ahrberg, and B. G. Chung, "Dual-neodymium magnet-based microfluidic separation device," *Sci Rep*, vol. 9, no. 1, p. 9502, 2019, ISSN: 2045-2322 (Electronic) 2045-2322 (Linking). DOI: 10.1038/s41598-019-45929-y.
- [103] T. Li, J. Chen, Y. Han, Z. Ma, and J. Wu, "Study on the characteristic point location of depth average velocity in smooth open channels: Applied to channels with flat or concave boundaries," *Water*, vol. 12, no. 2, 2020, ISSN: 2073-4441. DOI: 10.3390/w12020430.

- [104] A. Liakopoulos, F. Sofos, and T. E. Karakasidis, “Friction factor in nanochannel flows,” *Microfluidics and Nanofluidics*, vol. 20, no. 1, 2016, ISSN: 1613-4982. DOI: 10.1007/s10404-015-1699-5.
- [105] F. Liu, L. Ni, and J. Zhe, “Lab-on-a-chip electrical multiplexing techniques for cellular and molecular biomarker detection,” *Biomicrofluidics*, vol. 12, no. 2, p. 021501, 2018, ISSN: 1932-1058 (Print) 1932-1058 (Linking). DOI: 10.1063/1.5022168.
- [106] H. Y. Liu, C. Koch, A. Haller, S. A. Joosse, R. Kumar, M. J. Vellekoop, L. J. Horst, L. Keller, A. Babayan, A. V. Failla, J. Jensen, S. Peine, F. Keplinger, H. Fuchs, K. Pantel, and M. Hirtz, “Evaluation of microfluidic ceiling designs for the capture of circulating tumor cells on a microarray platform,” *Adv Biosyst*, vol. 4, no. 2, e1900162, 2020, ISSN: 2366-7478 (Print) 2366-7478 (Linking). DOI: 10.1002/adbi.201900162.
- [107] R. Liu, C. H. Chu, N. Wang, T. Ozkaya-Ahmadov, O. Civelekoglu, D. Lee, A. K. M. Arifuzzman, and A. F. Sarioglu, “Combinatorial immunophenotyping of cell populations with an electronic antibody microarray,” *Small*, vol. 15, no. 51, e1904732, 2019, ISSN: 1613-6829 (Electronic) 1613-6810 (Linking). DOI: 10.1002/smll.201904732.
- [108] J. Loureiro, C. Fermon, M. Pannetier-Lecoeur, G. Arrias, R. Ferreira, S. Cardoso, and P. P. Freitas, “Magnetoresistive detection of magnetic beads flowing at high speed in microfluidic channels,” *IEEE Transactions on Magnetics*, vol. 45, no. 10, pp. 4873–4876, 2009, ISSN: 0018-9464. DOI: 10.1109/tmag.2009.2026287.
- [109] M. Madadelahi, L. F. Acosta-Soto, S. Hosseini, S. O. Martinez-Chapa, and M. J. Madou, “Mathematical modeling and computational analysis of centrifugal microfluidic platforms: A review,” *Lab on a Chip*, vol. 20, no. 8, pp. 1318–1357, 2020, ISSN: 1473-0197. DOI: 10.1039/c9lc00775j.
- [110] R. P. McEver and C. Zhu, “Rolling cell adhesion,” *Annu Rev Cell Dev Biol*, vol. 26, pp. 363–96, 2010, ISSN: 1530-8995 (Electronic) 1081-0706 (Linking). DOI: 10.1146/annurev.cellbio.042308.113238.
- [111] D. P. McIntyre, A. Lashkaripour, and D. Densmore, “Rapid and inexpensive microfluidic electrode integration with conductive ink,” *Lab on a Chip*, 2020, ISSN: 1473-0197 1473-0189. DOI: 10.1039/d0lc00763c.
- [112] A. Munaz, M. J. A. Shiddiky, and N. T. Nguyen, “Recent advances and current challenges in magnetophoresis based micro magnetofluidics,” *Biomicrofluidics*,

- vol. 12, no. 3, p. 031501, 2018, ISSN: 1932-1058 (Print) 1932-1058 (Linking). DOI: 10.1063/1.5035388.
- [113] N.-T. Nguyen, "Micro-magnetofluidics: Interactions between magnetism and fluid flow on the microscale," *Microfluidics and Nanofluidics*, vol. 12, no. 1-4, pp. 1–16, 2011, ISSN: 1613-4982 1613-4990. DOI: 10.1007/s10404-011-0903-5.
- [114] N. Pamme, "Magnetism and microfluidics," *Lab Chip*, vol. 6, no. 1, pp. 24–38, 2006, ISSN: 1473-0197 (Print) 1473-0189 (Linking). DOI: 10.1039/b513005k.
- [115] J. W. Perthold and C. Oostenbrink, "Simulation of reversible protein–protein binding and calculation of binding free energies using perturbed distance restraints," *Journal of Chemical Theory and Computation*, vol. 13, no. 11, pp. 5697–5708, 2017, ISSN: 1549-9618 1549-9626. DOI: 10.1021/acs.jctc.7b00706.
- [116] A. Pierres, D. Touchard, A.-M. Benoliel, and P. Bongrand, "Dissecting streptavidin-biotin interaction with a laminar flow chamber," *Biophysical Journal*, vol. 82, no. 6, pp. 3214–3223, 2002, ISSN: 0006-3495. DOI: 10.1016/s0006-3495(02)75664-6.
- [117] M. Reisbeck, M. J. Helou, L. Richter, B. Kappes, O. Friedrich, and O. Hayden, "Magnetic fingerprints of rolling cells for quantitative flow cytometry in whole blood," *Scientific Reports*, vol. 6, no. 1, 2016, ISSN: 2045-2322. DOI: 10.1038/srep32838.
- [118] J. Schütt, R. Illing, O. Volkov, T. Kosub, P. N. Granell, H. Nhalil, J. Fassbender, L. Klein, A. Grosz, and D. Makarov, "Two orders of magnitude boost in the detection limit of droplet-based micro-magnetofluidics with planar hall effect sensors," *ACS Omega*, vol. 5, no. 32, pp. 20 609–20 617, 2020, ISSN: 2470-1343 2470-1343. DOI: 10.1021/acsomega.0c02892.
- [119] J. Schütt, D. I. Sandoval Bojorquez, E. Avitabile, E. S. Oliveros Mata, G. Milyukov, J. Colditz, L. G. Delogu, M. Rauner, A. Feldmann, S. Koristka, J. M. Middeke, K. Sockel, J. Fassbender, M. Bachmann, M. Bornhäuser, G. Cuniberti, and L. Baraban, "Nanocytometer for smart analysis of peripheral blood and acute myeloid leukemia: A pilot study," *Nano Letters*, 2020, ISSN: 1530-6984 1530-6992. DOI: 10.1021/acs.nanolett.0c02300.
- [120] F. Shamsipour, A. H. Zarnani, R. Ghods, M. Chamankhah, F. Forouzesh, S. Vafaei, A. A. Bayat, M. M. Akhondi, M. Ali Oghabian, and M. Jeddi-Tehrani, "Conjugation of monoclonal antibodies to super paramagnetic iron oxide nanoparticles for detection of her2/neu antigen on breast cancer cell lines," *Avicenna J*

Med Biotechnol, vol. 1, no. 1, pp. 27–31, 2009, ISSN: 2008-2835 (Print) 2008-2835 (Linking).

- [121] S. S. Shevkoplyas, A. C. Siegel, R. M. Westervelt, M. G. Prentiss, and G. M. Whitesides, “The force acting on a superparamagnetic bead due to an applied magnetic field,” *Lab Chip*, vol. 7, no. 10, pp. 1294–302, 2007, ISSN: 1473-0197 (Print) 1473-0189 (Linking). DOI: 10.1039/b705045c.
- [122] C. Sommer, “Die großenabhängigkeit der gleichgewichtsgeschwindigkeit von partikeln beim transport in mikrokanälen,” Thesis, 2014.
- [123] D. Song, R. K. Gupta, and R. P. Chhabra, “Drag on a sphere in poiseuille flow of shear-thinning power-law fluids,” *Industrial and Engineering Chemistry Research*, vol. 50, no. 23, pp. 13 105–13 115, 2011, ISSN: 0888-5885 1520-5045. DOI: 10.1021/ie102120p.
- [124] H. C. Tekin, M. Cornaglia, and M. A. Gijs, “Attomolar protein detection using a magnetic bead surface coverage assay,” *Lab Chip*, vol. 13, no. 6, pp. 1053–9, 2013, ISSN: 1473-0189 (Electronic) 1473-0189 (Linking). DOI: 10.1039/c3lc41285g.
- [125] A. E. Urusov, A. V. Petrakova, M. V. Vozniak, A. V. Zherdev, and B. B. Dzantiev, “Rapid immunoenzyme assay of aflatoxin b1 using magnetic nanoparticles,” *Sensors (Basel)*, vol. 14, no. 11, pp. 21 843–57, 2014, ISSN: 1424-8220 (Electronic) 1424-8220 (Linking). DOI: 10.3390/s141121843.
- [126] C. Wang, S. Zhao, X. Zhao, L. Chen, Z. Tian, X. Chen, and S. Qin, “A novel wide-range microfluidic dilution device for drug screening,” *Biomicrofluidics*, vol. 13, no. 2, p. 024 105, 2019, ISSN: 1932-1058 (Print) 1932-1058 (Linking). DOI: 10.1063/1.5085865.
- [127] H. Wang and Y. Wang, “Measurement of water flow rate in microchannels based on the microfluidic particle image velocimetry,” *Measurement*, vol. 42, no. 1, pp. 119–126, 2009, ISSN: 02632241. DOI: 10.1016/j.measurement.2008.04.012.
- [128] H. Watarai and M. Namba, “Capillary magnetophoresis of human blood cells and their magnetophoretic trapping in a flow system,” *Journal of Chromatography A*, vol. 961, no. 1, pp. 3–8, 2002, ISSN: 00219673. DOI: 10.1016/s0021-9673(02)00748-3.
- [129] R. Wirix-Speetjens, W. Fyen, X. Kaidong, B. Jo De, and G. Borghs, “A force study of on-chip magnetic particle transport based on tapered conductors,” *IEEE*

- Transactions on Magnetics*, vol. 41, no. 10, pp. 4128–4133, 2005, ISSN: 0018-9464. DOI: 10.1109/tmag.2005.855345.
- [130] D. Wu and J. Voldman, “An integrated model for bead-based immunoassays,” *Biosensors and Bioelectronics*, vol. 154, 2020, ISSN: 09565663. DOI: 10.1016/j.bios.2020.112070.
 - [131] T. Yago, J. Wu, C. D. Wey, A. G. Klopocki, C. Zhu, and R. P. McEver, “Catch bonds govern adhesion through I-selectin at threshold shear,” *Journal of Cell Biology*, vol. 166, no. 6, pp. 913–923, 2004, ISSN: 1540-8140. DOI: 10.1083/jcb.200403144.
 - [132] R. Yokokawa, Y. Sakai, A. Okonogi, I. Kanno, and H. Kotera, “Force measurement and modeling for motor proteins between microsphere and microfluidic channel surface,” ISBN: 978-0-9798064-3-8.
 - [133] T. Zhu, D. J. Lichlyter, M. A. Haidekker, and L. Mao, “Analytical model of microfluidic transport of non-magnetic particles in ferrofluids under the influence of a permanent magnet,” *Microfluidics and Nanofluidics*, vol. 10, no. 6, pp. 1233–1245, 2011, ISSN: 1613-4982 1613-4990. DOI: 10.1007/s10404-010-0754-5.
 - [134] N. Graf, E. Yeğen, A. Lippitz, D. Treu, T. Wirth, and W. E. S. Unger, “Optimization of cleaning and amino-silanization protocols for si wafers to be used as platforms for biochip microarrays by surface analysis (xps, tof-sims and nexafs spectroscopy),” *Surface and Interface Analysis*, vol. 40, no. 3-4, pp. 180–183, 2008, ISSN: 0142-2421. DOI: 10.1002/sia.2621.
 - [135] S. Magalhães, L. Alves, B. Medronho, A. C. Fonseca, A. Romano, J. F. Coelho, and M. Norgren, “Brief overview on bio-based adhesives and sealants,” *Polymers*, vol. 11, no. 10, p. 1685, 2019, ISSN: 2073-4360. DOI: 10.3390/polym11101685.
 - [136] J. V. Staros, “N-hydroxysulfosuccinimide active esters: Bis(n-hydroxysulfosuccinimide) esters of two dicarboxylic acids are hydrophilic, membrane-impermeant, protein cross-linkers,” *Biochemistry*, vol. 21, no. 17, pp. 3950–3955, 1982, PMID: 7126526. DOI: 10.1021/bi00260a008.
 - [137] Y. Eisenberg-Domovich, V. P. Hytönen, M. Wilchek, E. A. Bayer, M. S. Kulomaa, and O. Livnah, “High-resolution crystal structure of an avidin-related protein: insight into high-affinity biotin binding and protein stability,” *Acta Crystallographica Section D*, vol. 61, no. 5, pp. 528–538, May 2005. DOI: 10.1107/S0907444905003914.

Statement

I declare that I have authored this thesis independently, that I have not used other than the declared sources / resources, and that I have explicitly marked all material which has been quoted either literally or by content from the used sources.

Munich, December 4th, 2020, Signature